



**HAL**  
open science

## CFD analysis on the spatial effect of vortex generators in concentric tube heat exchangers – A comparative study

Rima Aridi, Samer Ali, Thierry Lemenand, Jalal Faraj, Mahmoud Khaled

### ► To cite this version:

Rima Aridi, Samer Ali, Thierry Lemenand, Jalal Faraj, Mahmoud Khaled. CFD analysis on the spatial effect of vortex generators in concentric tube heat exchangers – A comparative study. *International Journal of Thermofluids*, 2022, 16, pp.100247. 10.1016/j.ijft.2022.100247 . hal-03859016

**HAL Id: hal-03859016**

**<https://univ-angers.hal.science/hal-03859016>**

Submitted on 23 Jan 2024

**HAL** is a multi-disciplinary open access archive for the deposit and dissemination of scientific research documents, whether they are published or not. The documents may come from teaching and research institutions in France or abroad, or from public or private research centers.

L'archive ouverte pluridisciplinaire **HAL**, est destinée au dépôt et à la diffusion de documents scientifiques de niveau recherche, publiés ou non, émanant des établissements d'enseignement et de recherche français ou étrangers, des laboratoires publics ou privés.



Distributed under a Creative Commons Attribution - NonCommercial - NoDerivatives 4.0 International License



# CFD analysis on the spatial effect of vortex generators in concentric tube heat exchangers – A comparative study

Rima Aridi<sup>a</sup>, Samer Ali<sup>b</sup>, Thierry Lemenand<sup>a</sup>, Jalal Faraj<sup>c,d</sup>, Mahmoud Khaled<sup>c,e,\*</sup>

<sup>a</sup> LARIS EA 7315, Polytech Angers, University of Angers, Angers, France

<sup>b</sup> Univ. Lille, Institut Mines-Télécom, Univ. Artois, Junia, ULR 4515 – LGCgE, Laboratoire de Génie Civil et géo-Environnement, Lille, F-59000 France

<sup>c</sup> Energy and Thermo-Fluid Group, International University of Beirut BIU, Beirut, Lebanon

<sup>d</sup> Faculty of Technology, Lebanese University, Saida, Lebanon

<sup>e</sup> Energy and Thermo-Fluid Group, Lebanese International University LIU, Bekaa, Lebanon

## ARTICLE INFO

### Keywords:

CFD analysis  
Vortex generators  
Concentric tube heat exchanger  
Heat transfer  
Hot fluid  
Cold fluid  
Counterflow

## ABSTRACT

The present article is discussing the performance of heat transfer enhancement (HTE) using a trapezoidal vortex generator in a Concentric Tube Heat Exchanger (CTHE) through Computational Fluid Dynamics (CFD) code ANSYS Fluent. Heat transfer and fluid flow analysis are conducted for various Reynolds numbers inside the tube and annular. The effects of Vortex Generators (VGs) are studied as well, and the turbulence flow is simulated using the  $k-\omega$  model. The analysis was made on four designs, where the VGs are placed in three different locations as follows: (case 0) no VGs, (case 1) VGs inside the tube, (case 2) VGs on the interface between annular and tube, and (case 3) VGs on the outer wall of the annular part. Accordingly, the overall heat transfer, heat transfer ratio, and heat transfer/power of each of the three cases with VGs are normalized to case 0 to study the effect of VGs on the flow and heat transfer enhancement. Results show that VGs are effective in all locations and cases, however, the highest improvement was spotted in case 1 at Reynolds number of 8000 for the cold fluid and Reynolds number of 2000 for the hot water, where the enhancement of heat transfer ratio was 97% for case 1, 92% for case 2 and 56% for case 3, whereas the thermal enhancement factor was 210% for case 1, 180% for case 2 and 142% for case 3.

## 1. Introduction

Heat exchangers (HEs) are widely used in almost every process and manufacturing sector around the world [1,2], where two fluids are usually separated by a wall and heat is transferred from a hot fluid to a cold fluid at the same time using heat exchanger equipment. Generally, most HEs involve two-fluid, but three-fluid heat exchangers are becoming more common such as being employed in solar flat plate collector systems [3]. HEs are fabricated in a variety of flow configurations and designs, several types of HEs are categorized according to different applications such as finned, shell and tube, fixed HEs and many others [4,5]. However, the Concentric Tube Heat Exchanger (CTHE) or double pipe HE is the simplest in terms of design and cost [6], in which a pipe is inserted into another pipe and the two fluids each have their inlet and exit ducts. Then the heat is transferred from the hot fluid to the cold fluid through the inner tube wall, which is the interface between the annular and the tube. Both laminar and turbulent flow regimes can be

used in heat exchangers. Different applications, such as small multi-functional HX and tubular exchanger reactors, operate in the laminar flow regime [7,8]. However, some other applications require turbulent flow [9]. According to the flow arrangement, there are two types of flow arrangements: parallel flow and counterflow. In this study counterflow is employed since studies show that counterflow is more effective in terms of heat transfer [10,11]. So, warm fluid enters from one side and the cold fluid flows from the other opposite side as shown in Fig. 1.

CTHE is used in various applications in thermal and fluid domains such as heat recovery from oil cooling, desuperheating in refrigeration and air conditioning, engine cooling circuits, pharmaceutical industry, dairy, and chemical industry, refinery, etc. [6]. Thus, improving the overall performance of the HEs is fundamental for many industries. Enhancing heat transfer is a technique used for increasing the overall performance of HEs, where an increase or decrease in heat transfer holds a major role in energy manufacturers [12,13]. For instance, in several applications increasing the coefficient of convection heat transfer is

\* Corresponding author.

E-mail address: [mahmoud.khaled@liu.edu.lb](mailto:mahmoud.khaled@liu.edu.lb) (M. Khaled).

<https://doi.org/10.1016/j.ijft.2022.100247>

Received 30 August 2022; Received in revised form 29 October 2022; Accepted 7 November 2022

Available online 11 November 2022

2666-2027/© 2022 The Author(s). Published by Elsevier Ltd. This is an open access article under the CC BY-NC-ND license (<http://creativecommons.org/licenses/by-nc-nd/4.0/>).

essential due to cost limitations and space such as plasma reactors, cooling of electronic devices, gas turbine combustors, and turbine blades [6]. The convective heat transfer can be improved by enhancing the fluid flow velocity, enlarging the heat transfer area, and stimulating disturbance inflow using vortex generators, roughness, spiral springs, baffles, or tangential fluid injection [14,15].

There are three types of heat transfer enhancement methods: passive, active, and dynamic [16]. Active heat transfer enhancement techniques include vibration, electromagnetic field, and jet impingent, and are categorized as active since they involve an external source of power. The passive techniques are the most practical and efficient, they can be performed with treated surfaces, rough surfaces or grooves, and Vortex Generators (VGs) [17,18], which will be the focus of this research. The last type is the dynamic technique, it is efficient as well because flexible VGs are used [19,20].

Thus, inducing turbulence inflow is considered an effective method for heat transfer development, which is classified into active and passive systems. Active systems are the techniques that use the external power to enhance heat transfer, whereas passive systems are the techniques that do not require external power [21,22], however, they make benefit from the geometry to enhance heat transfer [23,24]. VG is one of the widely employed passive methods that increase the rate of heat transfer and thermal performance of HEs [25,26], without adding the cost of external power for inducing turbulence [27].

In this framework, the numerical simulations offer a prevailing design and optimization tool giving vision to the optimal parameters and design proposed as a settlement between best heat transfer improvement and energy spending [28]. In this study, a numerical analysis is held by comparing the enhancement of heat transfer in a Concentric Tube Heat Exchanger (CTHE) by employing Vortex Generators (VGs) in three different ways, then analyzing the results and building up a conclusion accordingly. Ansys Fluent is employed to visualize the behavior of fluid flow at different locations of VGs and different mass flows of both the hot and cold fluid. The aim of this study is to enhance the performance of CTHE, where enhancing its performance is the same as enhancing the overall performance of the applications that use CTHE. Moreover, this will create a more reliable heat transfer technique that saves more energy with simple geometrical modifications.

The novelty of this study is:

- 1- Studying the investigating the performance of CTHE through two aspects:
  - a- Analyzing the effect of the geometry which means changing the location of VGs in three different locations.
  - b- Varying the Reynolds number by changing the velocity in each region, where each case underwent 18 simulations. The simulation was by fixing the hot region in one value and changing that of the other region and so on until covering all the possibilities of the 6 values of  $Re$  number in the two regions.

- 2- Comparing the results obtained from two aspects:

- a- Maximum improvement to lowest improvement for each case, which means fixing geometry and comparing the effect of the velocity.
- b- Maximum improvement and lowest improvement for all the cases, which means varying the geometry and fixing the velocity.

- 3- Investigating the physical mechanisms behind the results obtained of maximum and minimum improvement values by:
  - a- Studying the location of vortices along the tube and
  - b- Obtaining the local value of the heat convection coefficient after and before each row of VGs.

## 2. Problem description

### 2.1. Mathematical formulation

In the following study, the flow goes through three-dimensional (3D) steady-state Reynolds averaged Navier-Stokes (RANS) equations. The continuity and momentum equations for an incompressible Newtonian fluid are as follows [29]:

$$\frac{\partial u_i}{\partial x_i} = 0 \tag{1}$$

$$u_j \frac{\partial u_i}{\partial x_j} = \frac{\partial p}{\partial x_i} + \nu \frac{\partial^2 u_i}{\partial x_j \partial x_j} - \frac{\overline{\partial u_i u_j}}{\partial x_j} \tag{2}$$

where the term  $\overline{u_i u_j}$  is the Reynolds stress due to the change of velocity.

Besides, the turbulent flow is considered wherever the shear-stress transport (SST)  $k - \omega$  model established by Menter [30] is employed, which are stated below [29]:

$$\rho \frac{\partial}{\partial x_i} (\omega u_i) = \frac{\partial}{\partial x_i} (\Gamma_k) \frac{\partial k}{\partial x_j} G_k - Y_k \tag{3}$$

$$\rho \frac{\partial}{\partial x_i} (\omega u_i) = \frac{\partial}{\partial x_j} (\Gamma_\omega) \frac{\partial \omega}{\partial x_j} G_\omega - Y_\omega + D_\omega \tag{4}$$

where  $G_k$  denotes the generation of turbulent kinetic energy owed to gradients of mean velocity.  $G_\omega$  signifies the generation of  $\omega$ .  $Y_k$  and  $Y_\omega$  signify the dissipation of  $k$  and  $\omega$  owed to turbulence and  $D_\omega$  denotes the cross-diffusion term. For the  $k - \omega$  model, the effective diffusivities  $\Gamma_k$  and  $\Gamma_\omega$  models are known as follows [29]:

$$\Gamma_k = \mu + \frac{\mu_t}{\sigma_k} \tag{5}$$

$$\Gamma_\omega = \mu + \frac{\mu_t}{\sigma_\omega} \tag{6}$$

where  $\sigma_k$  and  $\sigma_\omega$  represent the Prandtl numbers for  $k$  and  $\omega$  respectively, and  $\mu_t$  represents the turbulent viscosity. Heat transfer is represented in the equation below [29]:

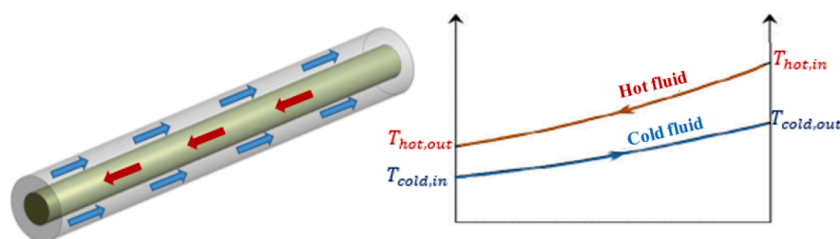


Fig. 1. Counter-flow heat exchanger with its temperature diagram.

$$\frac{\partial}{\partial x_i} [u_i (\rho E + p)] = \frac{\partial}{\partial x_i} \left( \lambda_{eff} \frac{\partial T}{\partial x_i} \right) \quad (7)$$

where  $E$  is the total energy and  $\lambda_{eff}$  the effective thermal conductivity.

In this study, the numerical simulations are held through the CFD code ANSYS Fluent [31]. The combination of pressure-velocity is created using the coupled algorithm, which determines the momentum and pressure-based continuity equations together. The flow equations are determined with twice accuracy and a second-order upwind design for spatial discretization of the convective forms [32]. The diffusion terms are central differenced and accurate to the second order. A convergence standard is established to  $10^{-6}$  for the results of the flow equations in Eqs. (1-4). However, a  $10^{-8}$  is placed for the result of the energy equation Eq. (7).

## 2.2. Computational domain

The computational domain for the simulations involves a Concentric Tube Heat Exchanger (CTHE) with three different arrangements of vortex generators (VG) to the inner and outer walls. The tube has a length  $L = 300$  mm, an inner diameter  $D_i = 20$  mm and an outer diameter  $D_o = 40$  mm. The dimensions taken in this study are not very important, since they can be changed according to the application, however, our concern is to understand the behavior of the flow under different conditions.

To enhance heat transfer, VGs of trapezoidal shape (big base = 6 mm, small base = 3 mm, height = 8 mm, and thickness = 1 mm) are employed with an inclined angle of  $30^\circ$  with the surface and directed opposite to flow direction. Six rows of four diametrically opposed VGs are inserted on the inner and outer walls which yield a total of 24 VGs in each case as shown in Fig. 2. The spacing between two consecutive rows of VGs is 30 mm. Four cases are considered, where in each case the Reynolds number of the flow in annular and tube varies as a result of changes in the mass flow rate  $\dot{m}$  of the fluid, which also affects the velocity as presented in the following equations [29]:

$$Re = \frac{4\dot{m}}{\pi (D_o + D_i)\mu} \quad (8)$$

$$V = \frac{\dot{m}}{\rho \cdot A} \quad (9)$$

where  $\mu$ ,  $\rho$ ,  $V$ , and  $A$  are the dynamic viscosity, density of water, velocity, and area normal to flow direction, respectively. Hot water passes through the tube at a temperature of  $30^\circ\text{C}$  (303 K), and cold-water flows through the annular at a temperature of  $20^\circ\text{C}$  (293 K), in a counter flow

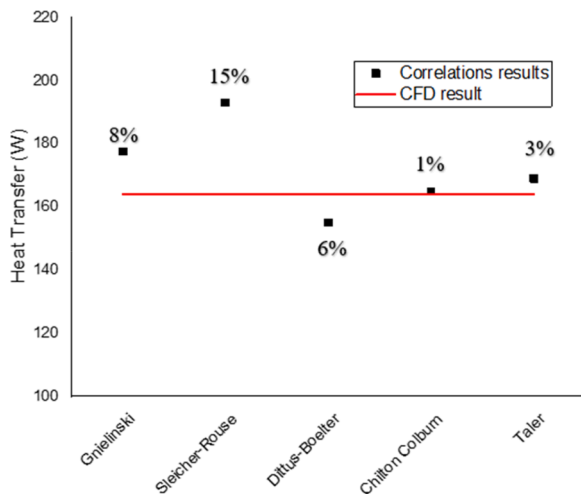


Fig. 2. Deviation of the result obtained in CFD to various correlations.

arrangement. The outer wall of the tube is adjusted to adiabatic with zero heat flux boundary condition.

## 2.3. System description and methodology

Numerical analysis is held by comparing the enhancement of heat transfer in a CTHE through employing Vortex Generators (VGs) in three different ways. Therefore, the simulation is done on four different cases, case 0: no VGs are employed and is considered the empty CTHE case, case 1: VGs are inserted into the inner wall of the tube, case 2: VGs are on the inner wall of the annular region, and case 3: VGs on the outer wall of the annular region as shown in Fig. 2. Case 0 is studied to compare each case of VG to that of the empty case.

In each case, the design is drawn on Ansys with a fixed temperature for both the hot and cold water with the temperature of hot and cold water for all the four cases are  $30^\circ\text{C}$  and  $20^\circ\text{C}$  respectively. Reynolds number of the hot and cold flow is varied through six values in laminar (500, 1000, and 2000) and turbulent (4000, 6000, and 8000) regimes, which affects the other input variables, such as mass flow rate, heat capacity, and heat transfer. The working fluid is water which determines the values of the fluid properties input such as thermal conductivity, specific heat, density. Consequently, this variation will result in different output performance parameters (Nusselt number, overall heat transfer ratio, required power...) for each value of the  $Re$  number. These parameters are normalized to case 0 to study the improvement of each case to no VG case and to perform a comparison among the three cases.

## 2.4. Numerical validation

To validate the results obtained from the CFD, validation test is done to study the accuracy and identify the deviation of the numerical simulations with respect to the correlations. Thus, the heat transfer ( $q$ ) was calculated through different correlation methods [33,34] and then compared to the result of  $q$  obtained in CFD. The results are shown in Fig. 3. Here it is noticed that the deviation of the CFD results differ from correlation to another in a range between +15% and -6%, with two deviations lower than 3%. These results are acceptable, and confirm the validation of the carried out numerical simulations.

## 2.5. Mesh sensitivity study

A mesh with polyhedral cells is applied for all the simulations. An independent study for the mesh is studied at  $Re = 8000$  for both hot and cold flow since 8000 is the highest Reynolds number. For the cases where VGs are presented, the mesh is refined at the VGs, at the inner wall separating the two fluids and at the outer wall of the annular region. Table 1 shows mesh sensitivity analysis, where three configurations of mesh were employed. The mesh is refined by decreasing the size of the element cells until the variation of heat transfer reaches 1%. The heat transfer rate between hot and cold-water streams  $q$  is calculated under three different mesh sizes, which are presented in the fourth column, then the deviation in heat transfer is done through the following equation, where “ $i$ ” is the mesh number. Near wall regions, fifteen mesh layers are chosen, and the height of the first grid point is minutely picked so that the resulting  $y^+$  value does not exceed 1 in all the used meshes. The chosen mesh for all the simulations is the mesh in case 2 with a total of 3651,456 elements, a maximum element size of 0.7 mm and a first inflation layer height of 0.01 mm.

## 3. Results and discussions

### 3.1. Performance parameters

The performance of different configurations is evaluated based on several parameters. In this section, the important parameters for global analysis are presented.

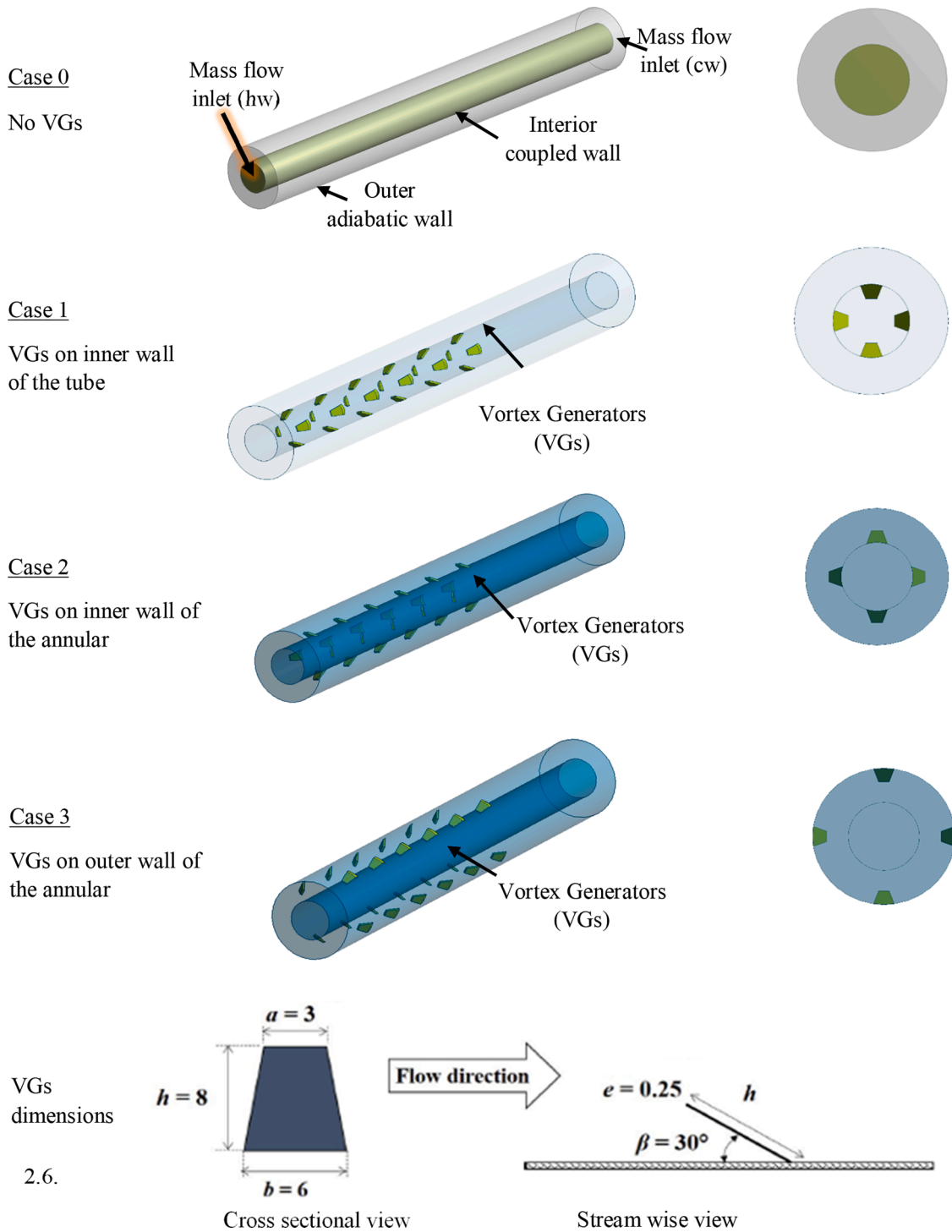


Fig. 3. Computational domain for all the four cases investigated displaying the boundary conditions, the VGs position and the dimensions of the trapezoidal shape VG (in mm).

Table 1  
Mesh sensitivity details.

Mesh	Maximum element size (mm)	Number of elements	Heat transfer $q$ (W)	$q$ deviation (%)
1	1.5	2089,201	239.811	6.58
2	0.7	3651,456	255.586	1.00
3	0.5	7020,216	258.143	-

The global friction factors for the tube and the annular regions are given by [29]:

$$f_{\text{tube}} = \frac{D_i}{l} \frac{\Delta P_{hw}}{0.5 \cdot \rho \cdot (V_{hw,i})^2} \quad (10)$$

$$f_{\text{annular}} = \frac{D_o - D_i}{l} \frac{\Delta P_{cw}}{0.5 \cdot \rho \cdot (V_{cw,i})^2} \quad (11)$$

where  $l$  is the length of the tube = 0.3 m,  $\rho$  is the density of the water,  $\Delta P$

is the pressure drop between the inlet and outlet flow where:  $\Delta P_{hw} = P_{inlethw} - P_{outlethw}$  is the pressure drop across the tube region with circulating hot water hence the subscript *hw*. Similarly, the pressure drop in the annular region is  $\Delta P_{cw} = P_{inletcw} - P_{outletcw}$ , with circulating cold water hence the subscript *cw*.  $V_{cw,i}$  and  $V_{hw,i}$  are the velocities at inlet cold water (cw) and hot water (hw) respectively.

To calculate the heat transfer rates between the hot and cold water, the following parameters are presented [29]:

$$q_{cw} = \dot{m}_{cw} \cdot Cp \cdot (T_{c,o} - T_{c,i}) \quad (12)$$

$$q_{hw} = \dot{m}_{hw} \cdot Cp \cdot (T_{h,i} - T_{h,o}) \quad (13)$$

where  $q_{cw}$  is the heat transfer of the cold water,  $q_{hw}$  is the heat transfer of the hot water,  $\dot{m}$  is the mass flow rate,  $Cp$  is the specific heat capacity of the water,  $T_{c,i}$  is the temperature of cold water at the inlet,  $T_{c,o}$  is the temperature of cold water at the outlet,  $T_{h,i}$  is the temperature of hot water at the inlet and  $T_{h,o}$  is the temperature of hot water at the outlet. Here the heat transferred from the hot water is totally gained by the cold water and as a result  $q_{cw} = q_{hw}$ .

The heat transfer convection coefficients for the common wall interface between the hot water and the cold water are given by [29]:

$$h_{hw} = \frac{q_{hw}}{\pi \cdot D_i \cdot l \cdot (\bar{T}_{hw} - \bar{T}_w)} \quad (14)$$

$$h_{cw} = \frac{q_{cw}}{\pi \cdot D_i \cdot l \cdot (\bar{T}_w - \bar{T}_{cw})} \quad (15)$$

where  $\bar{T}_w$  is the average temperature of the wall interface between the hot tube and cold annular,  $\bar{T}_{hw}$  is the arithmetic mean temperature of the hot water between the inlet and the outlet of the tube and is given by  $(\frac{T_{hw,i} + T_{hw,o}}{2})$ ,  $\bar{T}_{cw}$  is also the arithmetic mean temperature between the inlet and outlet of the annular side and is  $(\frac{T_{cw,i} + T_{cw,o}}{2})$  and finally  $D_i$  is the inner diameter of the tube.

To assess the enhancement in heat transfer, the global Nusselt numbers are calculated based on the tube side  $Nu_{tube}$  and the annular side  $Nu_{annular}$  and are given by [29]:

$$Nu_{annular} = \frac{h_{cw} \cdot (D_o - D_i)}{k} \quad (16)$$

$$Nu_{tube} = \frac{h_{hw} \cdot D_i}{k} \quad (17)$$

By neglecting the wall thermal resistance due to conduction, the overall heat transfer coefficient is calculated by [29]:

$$U = \frac{1}{\frac{1}{h_{annular}} + \frac{1}{h_{tube}}} \quad (18)$$

In all four cases, Reynolds numbers of the hot and cold flow are changed through six values: in laminar regime (500, 1000, 2000) and turbulent regime (4000, 6000, 8000) which will yield a total of 36 simulations performed to study all different possibilities.

To assess the thermal performance of vortex generators compared to the empty case, case 0 referred hereafter with index 0, additional parameters are defined and are explained as follows [29]:

- Overall heat transfer ratio: defines the ratio of  $U$  value for the VG cases to the  $U$  value of the empty case  $U_0$  and is equal to  $U / U_0$ .
- Heat transfer ratio: quantifies the enhancement in heat transfer rate  $q$  when adding VGs compared to the empty case  $q_0$ , equal to  $q / q_0$ .
- Pumping power ratio: is the ratio of the pumping power for the VG case relative to the empty case, and is equal to  $\frac{P}{P_0} = \frac{(\Delta P_{hw} \cdot \dot{m}_{hw} + \Delta P_{cw} \cdot \dot{m}_{cw})}{(\Delta P_{hw,0} \cdot \dot{m}_{hw,0} + \Delta P_{cw,0} \cdot \dot{m}_{cw,0})}$ .

where  $P$  is the pumping power input to get a specific Reynolds number in each of the cases 1, 2, or 3, and  $P_0$  is the pumping power input in case 0 that means the empty case with no VGs in both regions. The power input is calculated through the following equation  $P = \frac{\text{delta pressure}_{hw} \cdot \dot{m}_{hw} + \text{delta pressure}_{cw} \cdot \dot{m}_{cw}}{\rho}$ .

- Thermal enhancement factor (TEF): quantifies the relative enhancement in heat transfer to the increase in pumping power, which is the input power that is employed to run the flow when adding VGs. TEF is the ratio of heat transfer ratio and pumping power ratio:  $TEF = \frac{q/q_0}{P/P_0}$ .

### 3.2. Global analysis

After obtaining the main parameters, a comparison between the three cases was held to study the effect of the trapezoidal VGs on the performance of the heat transfer, input power, and thermal enhancement factor. Fig. 4 shows the variation of each of the above main parameters versus the Reynolds number of the hot and cold flow for the three cases studied.

As observed, the normalized overall heat transfer is greater than one through all the range of Reynolds numbers for hot and cold water, this indicates that the heat is always enhanced as compared to the empty VGs case. Besides, it is noticed from Fig. 4 that case 1 has the highest improvement value in all the three parameters, where the ratio in each parameter was highest at case 1. For instance,  $U/U_0$  displays a maximum improvement at low  $Re_{hw}$  and high  $Re_{cw}$ , however for cases 2 and 3,  $U/U_0$  displays a maximum improvement at high  $Re_{hw}$  and low  $Re_{cw}$ , where the maximum improvements compared to the empty case is 167% for case 1, 97% for case 2 and 58% for case 3.

Whereas the enhancement of  $U/U_0$  for case 1 is lowest at high  $Re_{hw}$  and  $Re_{cw}=4000$ , however for cases 2 and 3,  $U/U_0$  is lowest at water low  $Re_{hw}$  and high  $Re_{cw}$ . The minimum improvements compared to the empty case is 19.7% for case 1, 14.3% for case 2 and 9.4% for case 3. The difference in the optimum and minimum positions between the cases 1, 2 and 3 are attributed to two criteria: (1) the geometry corresponding to the tube, annular, and VGs, (2) the Reynolds number of the flow in each of the tube and the annular.

Similarly, the normalized heat transfer is greater than one for all the range of Reynolds numbers, which indicates the heat is enhanced as compared to the empty VGs case. For case 1,  $q/q_0$  displays a maximum improvement at low  $Re_{hw}$  and high  $Re_{cw}$ , however for cases 2 and 3,  $q/q_0$  displays a maximum improvement at high  $Re_{hw}$  and low  $Re_{cw}$ . The maximum improvements compared to the empty case are 97% for case 1, 92% for case 2 and 56% for case 3.

Whereas the enhancement of heat transfer ratio for case 1 is lowest at high  $Re_{hw}$  ( $=8000$ ) and low  $Re_{cw}$  ( $=2000$ ), however for cases 2 and 3,  $q/q_0$  is lowest at low  $Re_{hw}$  and high  $Re_{cw}$ , where the improvements compared to the empty case are 7.4% for case 1, 13% for case 2 and 5.4% for case 3.

However, a third main parameter should be also studied which is the thermal enhancement factor. Fig. 4 shows the variation of thermal enhancement factor versus Reynolds number. It is noticed that there are some places where this parameter is less than one which means that it is not efficient for all values of  $Re$ .

For case 1, thermal enhancement factor displays a maximum improvement at low  $Re_{hw}$  ( $=2000$ ) and high  $Re_{cw}$  ( $=8000$ ), however for cases 2 and 3, thermal enhancement factor displays a maximum improvement at high  $Re_{hw}$  ( $=8000$ ) and low  $Re_{cw}$  ( $=2000$ ). The maximum thermal enhancement factor reaches around 210% for case 1, 180% for case 2 and 142% for case 3.

Whereas the values of thermal enhancement factor for case 1 is lowest at high  $Re_{hw}$  ( $=8000$ ) and low  $Re_{cw}$  ( $=2000$ ), however for cases 2 and 3, thermal enhancement factor is lowest at low  $Re_{hw}$  and high  $Re_{cw}$ .

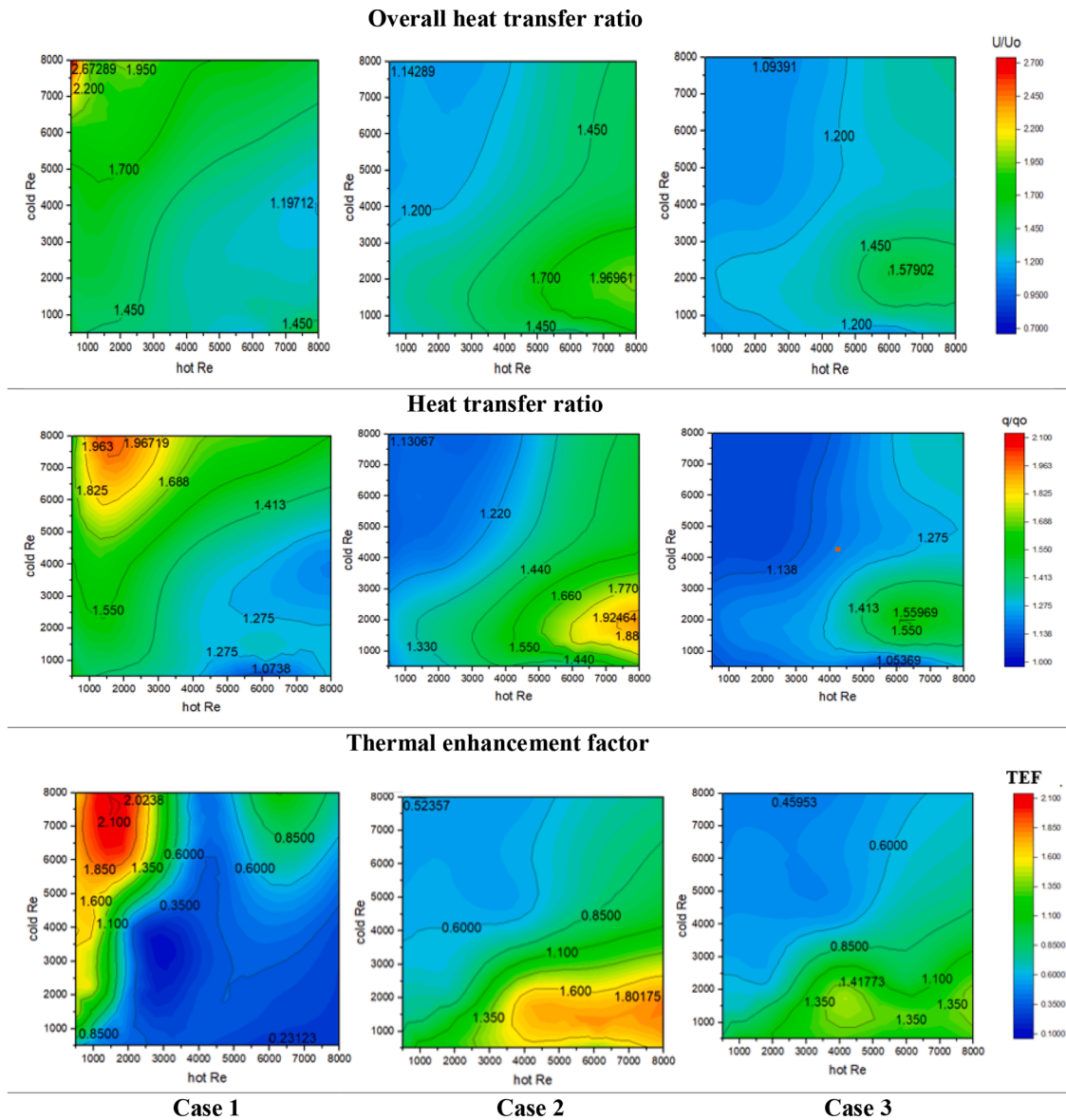


Fig. 4. Comparison between the main parameters for the three cases: case 1, case 2, and case 3.

The minimum thermal enhancement factor decreases compared to the empty case to 23% for case 1, 52.3% for case 2 and 45.9% for case 3.

As a conclusion from the above graphs the following points were noticed:

- Case 1 has the highest improvement of heat transfer among all cases to heat enhancement, and overall heat transfer.
- The highest improvement in case 1 was at low  $Re_{hw}$  (=2000) and high  $Re_{cw}$  (=8000). However, the lowest improvement was at high  $Re_{hw}$  (=6000 and 8000) and low  $Re_{cw}$  (=500, 2000, and 1000).
- On contrary, case 2 and case 3 exhibit the highest improvement at high  $Re_{hw}$  (=8000) and low  $Re_{cw}$  (=2000), which is opposite to case 1 that is because in cases 2 and 3, VGs are placed in the annular, however, in case 1 VGs are placed in the tube, then this could be attributed to the reason that creating turbulence in both regions increase the heat transfer more than having turbulence in one region, where in cases 2 and 3 both regions were turbulent, the hot region due to the high Reynolds number and the cold region due to the presence of VGs, which makes heat transfer optimum. Similarly, for

case 1, optimum heat transfer was in the presence of turbulence in both regions.

- Case 2 shows higher improvement than case 3 although in both cases VGs are presented in the annular, this is due to the location of VGs on the outer side of the annular: in fact, the outer wall is under adiabatic conditions so heat cannot be transferred, however at the interface between hot region and cold region the heat may be transferred much more efficiently.

### 3.3. Flow structure and temperature contours

In this section, a comparison is held at the locations where the highest improvement and lowest improvement occurred to find the reason behind the enhancements of each case. The comparison is done by analyzing the temperature, and vortices profile contour of each case on seven different planes located at 35, 65, 95, 125, 155, 185, and 250 mm (basically after each row of VGs) as shown in Fig. 5.

In this section, a closer analysis on the highest and lowest improvement of cases 1 and 2 is held to find the reason behind this difference within the same case. Case 3 does not show interesting results

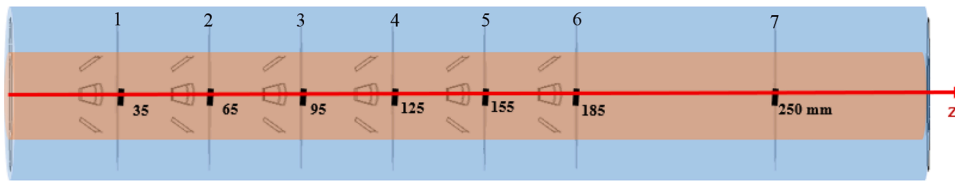


Fig. 5. The location of the seven planes in the CTHE.

as in cases 1 and 2 so the observation and analysis are done just on the highest improvement Reynolds number condition.

3.3.1. Temperature profiles for case 1

Fig. 6 and Fig. 7 show the temperature distribution along the CTHE of case 1 after each row of VGs at Reynolds numbers ( $Re_{hw}=2000 - Re_{cw}=8000$ ) and ( $Re_{hw}=8000 - Re_{cw}=2000$ ) respectively.

As noticed in Fig. 6, the temperature of the flow seems to be affected by the cooling process, where the outlet hot temperature decreases around 3 this was noticed in the change of contour, where after each row of VGs the temperature was changing not just at the wall and around the VGs, however at the center of the tube as well.

On contrary, in Fig. 7 the temperature decreases slightly, even with the presence of the VGs in the tube. Thus, the reason for this contradiction is due to the high Reynolds number in the tube and the low Reynolds number in the annular. The high Reynolds number in the annular creates a flow structure that reduces the thermal boundary layer as shown in Fig. 6. However, throughout all the contours in Fig. 7, a considerable thermal boundary layer is noticed around the wall in the annular, which is presented due to the low turbulence of the flow in the annular, this layer negatively affects the heat transfer. In other words, the heat is transferred to just the layer close to the boundary.

This explains that the Reynolds numbers condition ( $Re_{hw}=2000 - Re_{cw}=8000$ ) has higher heat transfer, which could be attributed to the flow structure. In the next section, vortical structures are presented to explain the association between flow and heat transfer performances.

3.3.2. Vortices profiles for case 1

Lambda2 method is a vortex core line identification algorithm [35] that can effectively detect vortices from a 3D fluid velocity field as shown in Fig. 8 and Fig. 9, where the vortices profiles of case 1 was detected after each row of VGs at the operating conditions ( $Re_{hw}=2000 - Re_{cw}=8000$ ) and ( $Re_{hw}=8000 - Re_{cw}=2000$ ) respectively.

Fig. 8 shows that vortices are located around the VGs where each VG generated two vortices, the vorticity decreases gradually towards the center. Besides, it is noticed that the intensity of vorticity slightly increased after contour 1, as a result of the increase in the velocity vectors. After contour 2, the behavior of the flow was approximately the same, however, at row 7, the behavior was obviously different, where the intensity of the vortices was less than the previous contours and velocity vectors of the flow were low.

Similarly for Fig. 9, the vortices are detected around the VGs and the behavior of the flow is almost the same from contour 2 till 6, however the intensity of the VGs was extremely high then it sharply decreased. This could be attributed to the high velocity and the presence of VGs at the same time, where high turbulence due to high Reynolds number with the presence of VGs may cause the vortices to swirl extremely around the VGs. At contour 7, the velocity vectors decreased with lower turbulence of the flow.

This difference between contour 7 and the previous ones in Figs. 8 and 9 confirms the effect of the VGs row along the tube.

3.3.3. Temperature profiles for case 2

Fig. 10 and Fig. 11 show the temperature profiles of case 2 after each row of VGs at the operating conditions ( $Re_{hw}=8000 - Re_{cw}=2000$ ) and ( $Re_{hw}=2000 - Re_{cw}=8000$ ) respectively.

As noticed in Fig. 10, the increase in temperature in the annular is noticeable, where the temperature of the cold fluid is increased by around 2.5, due to the turbulence in the tube from the high Reynolds number and the vorticity in the annular created by the VGs. The presence of turbulence in the heat water and the occurrence of vortices in the cold water increases the temperature difference at the thermal boundary layer, consequently enhancing the heat transfer. On the other side, heat transfer in Fig. 11 is low, this is represented by the thermal boundary layer in the tube which is a result of the laminar flow in the heat water. So to enhance the heat transfer, the flow must be turbulent which helps

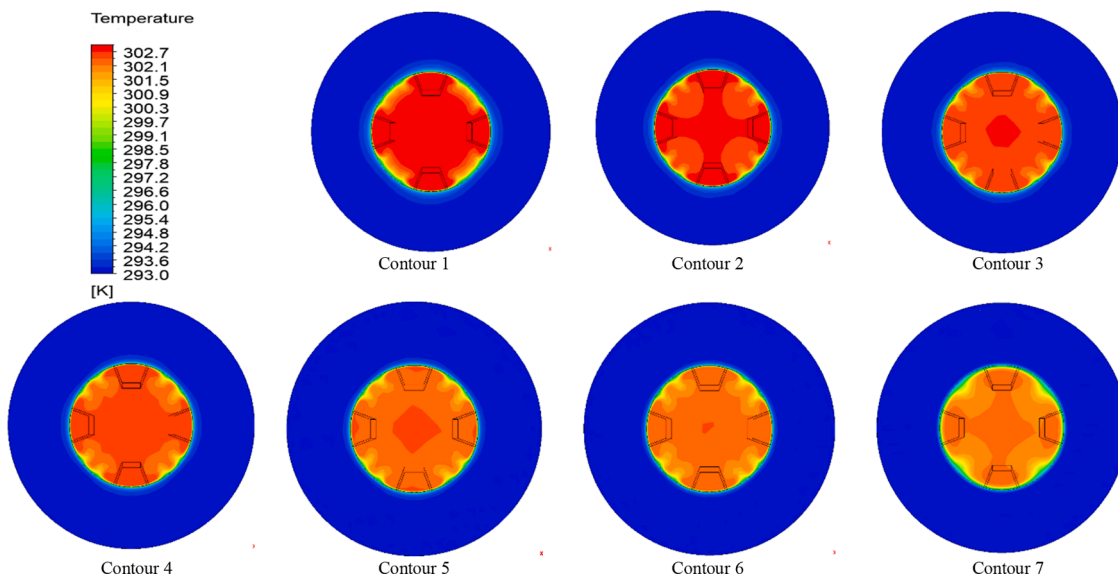


Fig. 6. Temperature profiles of case 1 for  $Re_{hw}=2000 - Re_{cw}=8000$ .

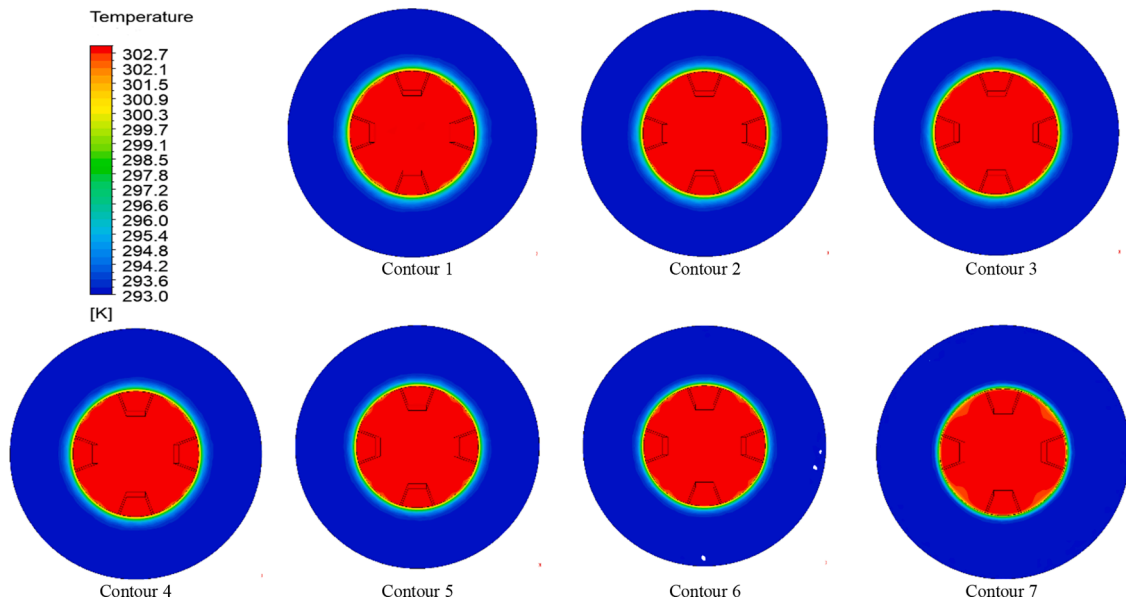


Fig. 7. Temperature profiles of case 1 for  $Re_{hw}=8000 - Re_{cw}=2000$ .

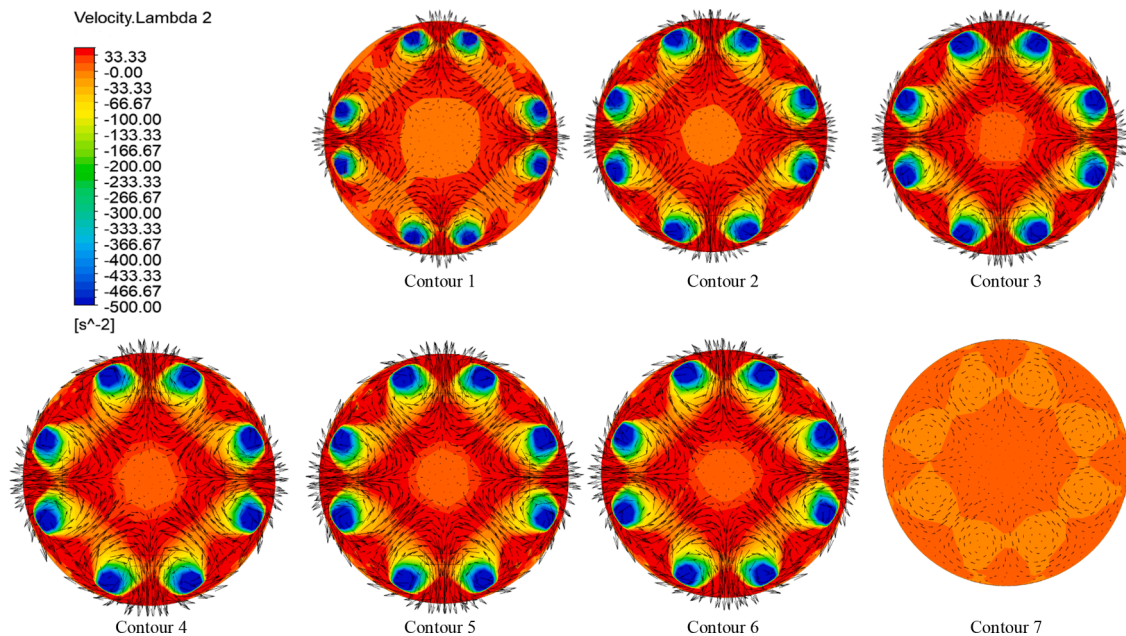


Fig. 8. Vortices profiles for case 1 for  $Re_{hw}=2000 - Re_{cw}=8000$ .

in mixing the fluid and getting a homogeneous temperature. This explains that the condition ( $Re_{hw}=8000 - Re_{cw}=2000$ ) has higher heat transfer.

### 3.3.4. Vortices profiles for case 2

Fig. 12 and Fig. 13 show the vortices profiles of case 2 after each row of VGs at Reynolds numbers ( $Re_{hw}=8000 - Re_{cw}=2000$ ) and ( $Re_{hw}=2000 - Re_{cw}=8000$ ) respectively.

Fig. 12 and Fig. 13 show that by provoking the cold flow with VGs, vortices are generated in the annular with each VG generating two vortices. Besides, it is noticed that the intensity of vortices was increasing after each row of VG along the tube until the last row (row 7), where the vortices were decreased significantly, which approves the effect that VGs have on the flow. Furthermore, in Fig. 12 the vortices in the annular are relatively low, however, in Fig. 13 the intensity of

vorticity was extremely high as a result of high velocity and high Reynolds number. In row 7, the vortices were decreased gradually so that the flow leaves the tube with lower turbulence.

### 3.3.5. Temperature and vortices profiles for case 3

Fig. 14 and Fig. 15 show the temperature profiles and vorticity profiles of case 3 after each row of VGs at the operating condition ( $Re_{hw}=8000 - Re_{cw}=2000$ ). As mentioned previously, case 3 did not show interesting results as in case 1 and 2, so the observation was done just on the more favorable conditions of Reynolds numbers.

For case 3, although the turbulence occur in both regions, in the annular due to the presence of VGs and in the tube due to the high Reynolds number, however the temperature did not change as much as in case 1 or case 2, since the temperature change did not exceed 0.5 as shown in Fig. 14. So, employing VGs on the outer side of the annular

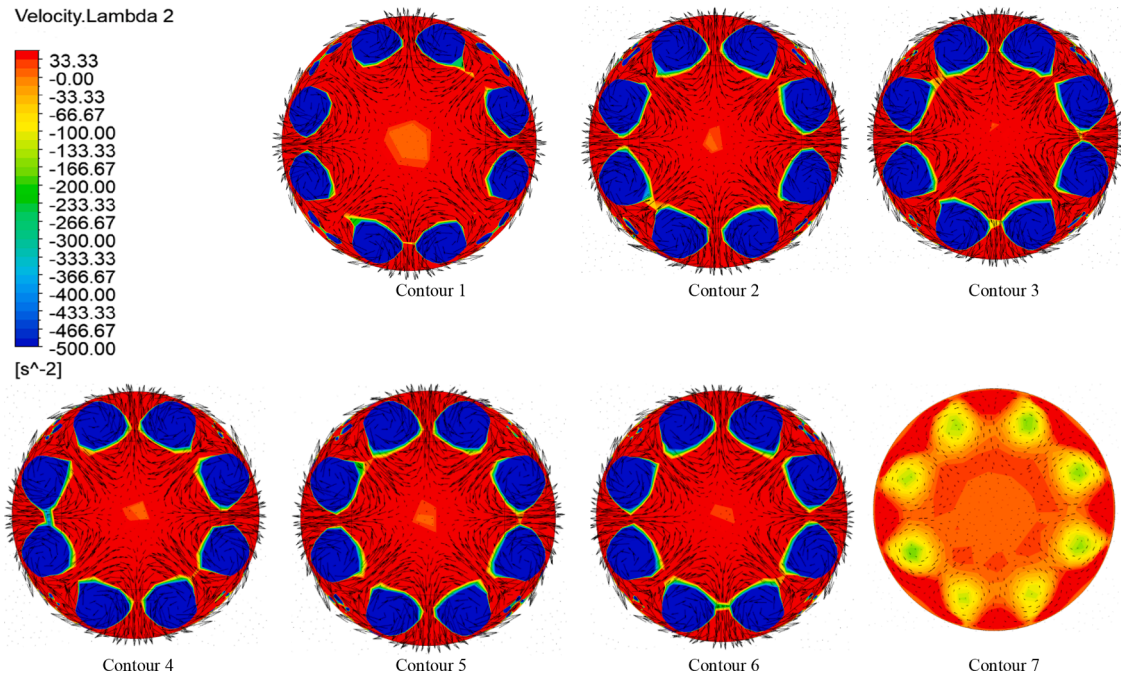


Fig. 9. Vortices profiles for case 1 for  $Re_{hw}=8000 - Re_{cw}=2000$ .

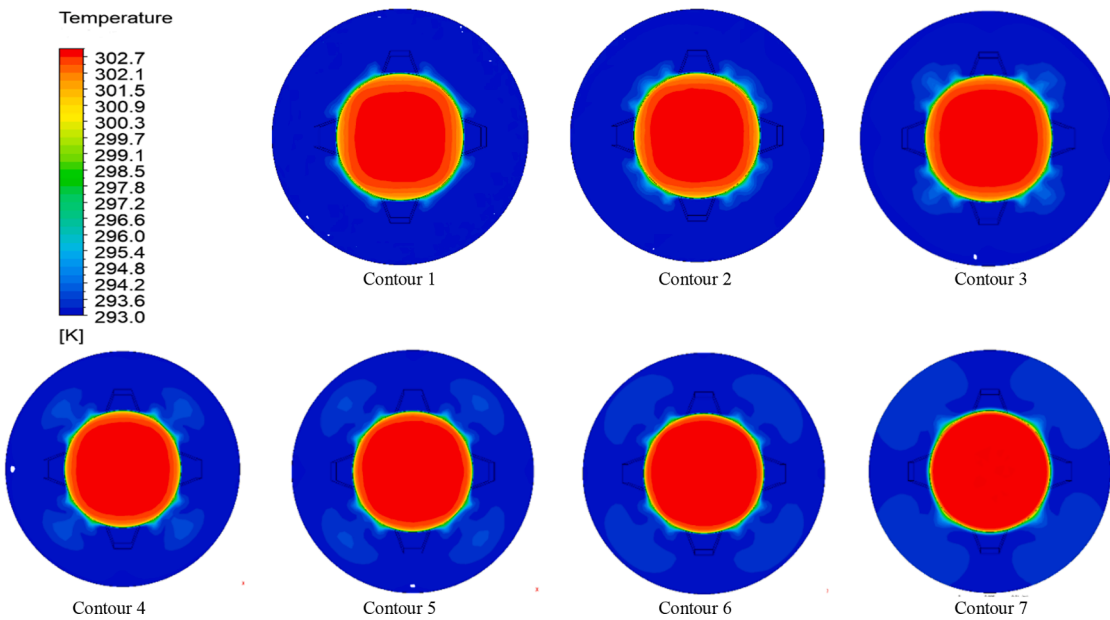


Fig. 10. Temperature profiles of case 2 for  $Re_{hw}=8000 - Re_{cw}=2000$ .

appears not efficient. Fig. 15 shows that vortices are around the VGs, which are closer to the outer wall (adiabatic part) and not to the interface wall between the annular and the tube where the heat is transferred, this makes the presence of VGs in case 3 not very effective as compared to case 1 and case 2.

#### 4. Evolution of vortices

In this section, the evolution of the vorticity is studied in each of the three cases (case 1, case 2, and case 3) at the highest and lowest improvement conditions. Thirteen planes were created along the Concentric Tube Heat Exchanger as shown in Fig. 16, where the z-axis shows the location of each plane along the tube and annular, and the y-

axis shows the height which is the diameter of the tube and the annular.

As noticed in Fig. 16, the planes are created before and after the VGs to investigate the effect of each row of VG on the evolution of the vortices. The study of vorticity is done on the three configurations of VGs: case 1, case 2, and case 3. Fig. 17 shows the evolution of the vortices along the tube, where the location of the center of vorticity was spotted at each plane and drawn to the y-axis. As observed from the graph in Fig. 17, the evolution of vorticity at case 1 was close to the interface annular tube wall at each row of VG, however, the vortices are directed to the center of the tube when it goes away from the VG row. For instance, at first row of VG (35 mm), the vortices were directed towards the wall of the tube 8 mm and 7.7 mm away from the center for  $Re_{hw}=2000 - Re_{cw}=8000$  and  $Re_{hw}=8000 - Re_{cw}=2000$  respectively.

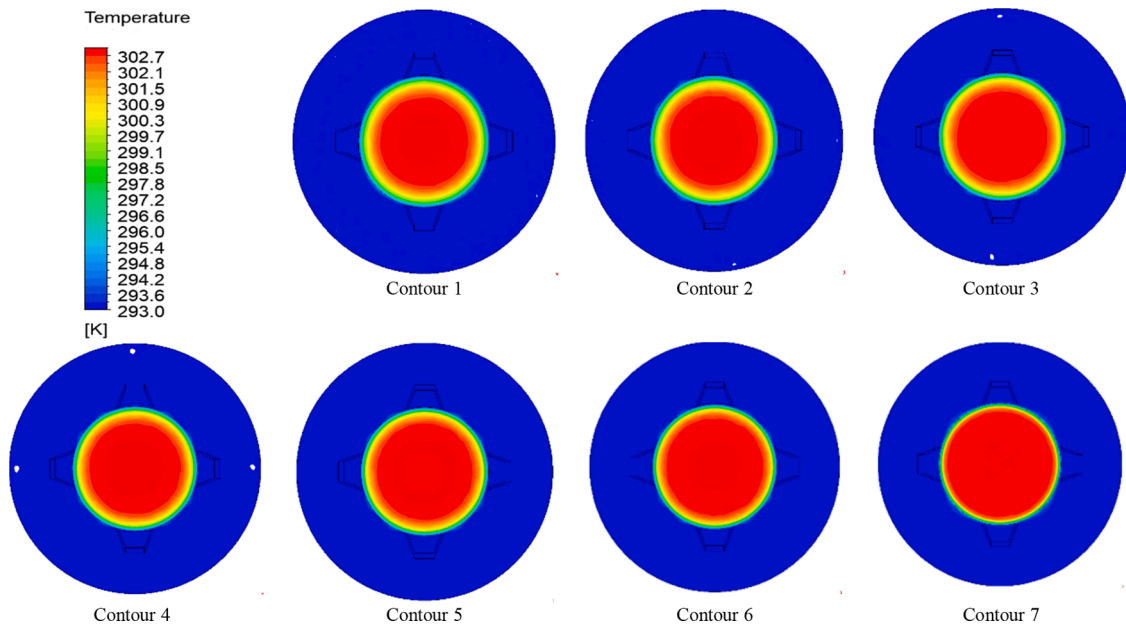


Fig. 11. Temperature profiles of case 2 for  $Re_{hw}=2000 - Re_{cw}=8000$ .



Fig. 12. Vorticity profiles of case 2 for  $Re_{hw}=8000 - Re_{cw}=2000$ .

Whereas, after the first row of VGs the vorticities were directed to the center with lower values 5.9 mm and 5.51 mm away from the center for  $Re_{hw}=2000 - Re_{cw}=8000$  and  $Re_{hw}=8000 - Re_{cw}=2000$  respectively. At 250 mm in the z-direction, which is 80 mm away from the last row of VG, the vorticity reaches 5.4 mm away from the central axis of the tube for the  $Re_{hw}=8000 - Re_{cw}=2000$ , and 6.1 mm away from the central axis of the tube for the  $Re_{hw}=2000 - Re_{cw}=8000$ .

Now for case 2, the evolution of vorticity was close to the interface\_annular\_tube wall at each row of VG, however, the vortices are directed towards the outer wall when it goes away from the VG row. For instance, at first row of VG (35 mm), the vortices were close to the interface\_annular\_tube wall 0.011 mm away from the center for both  $Re_{hw}=2000 - Re_{cw}=8000$  and  $Re_{hw}=8000 - Re_{cw}=2000$ . Whereas, after the first row of VGs the vorticities go up towards the outer wall with

values 0.012 mm and 0.013 mm away from the center for  $Re_{hw}=2000 - Re_{cw}=8000$  and  $Re_{hw}=8000 - Re_{cw}=2000$  respectively. At 250 mm in the z-direction, the vorticity reaches 0.014 mm away from the central axis of the tube for both  $Re_{hw}=2000 - Re_{cw}=8000$  and  $Re_{hw}=8000 - Re_{cw}=2000$ .

As for case 3, the evolution of vorticity was close to the outer wall at each row of VG, however, the vortices are directed downwards when it goes away from the VG row. For instance, at first row of VG (35 mm), the vortices were directed towards the outer wall of the tube 0.0178 mm and 0.0182 mm away from the center for  $Re_{hw}=2000 - Re_{cw}=8000$  and  $Re_{hw}=8000 - Re_{cw}=2000$  respectively. Whereas, after the first row of VGs the vorticities were directed downwards with lower values 0.0157 mm away from the center for both  $Re_{hw}=2000 - Re_{cw}=8000$  and  $Re_{hw}=8000 - Re_{cw}=2000$ . At 250 mm in the z-direction, the vorticity reaches 0.0131 mm away from the central axis of the tube for the  $Re_{hw}=2000 -$

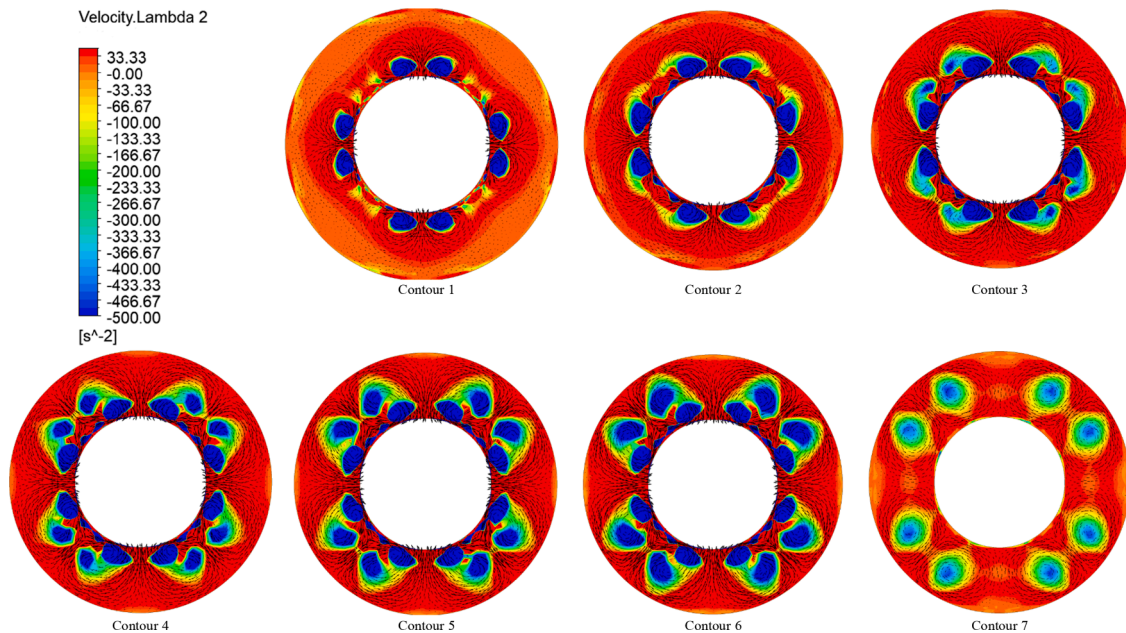


Fig. 13. Vortices profiles of case 2 for  $Re_{hw}=2000 - Re_{cw}=8000$ .

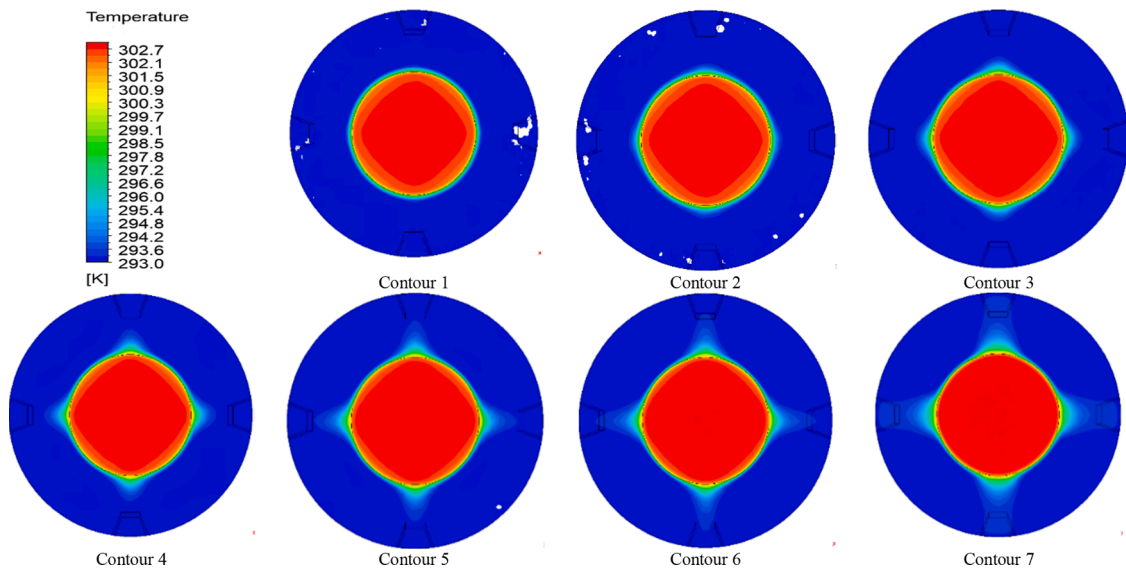


Fig. 14. Temperature profiles of case 3 for  $Re_{hw}=8000 - Re_{cw}=2000$ .

$Re_{cw}=8000$ , and 0.0129 mm away from the central axis of the tube for the  $Re_{hw}=8000 - Re_{cw}=2000$ .

As noticed, in the cases 1 and 2 the vorticity goes up at each row of VG and down away from VG rows. On contrary, case 2 witnessed low value at each row of VG and higher value away from VG rows. This could be due to the presence of VGs in case 2 that generate vortices upwards, while the cases 1 and 3 the VGs generate vortices that go downwards.

Fig. 18 shows the local overall heat transfer normalized to the case with no VG along the tube. In all cases, it is noticed that the values after each row of VG are higher than one, i.e. there exists an enhancement of the heat transfer compared to case with no VG. For case 1, the improvement is the highest among all the cases, and for the case 3, the improvement is the lowest.

Besides, it is noticed that for each case at the entrance of the tube (10 mm) the enhancement of heat transfer is null because there is no VG, so it is the same as the CTHE without VG. As soon as the fluid reaches the first row of VG, the improvement is noticed in all cases. After 185 mm of

the tube for each case, the enhancement is noticeably decreased, due to the absence of VGs.

Besides, it is noticed that the values of the local  $U/U_0$  graph in Fig. 18 match the values of overall  $U/U_0$  in Fig. 4, where case 1 exhibits the highest value at the operating conditions ( $Re_{hw}=2000 - Re_{cw}=8000$ ) of around 1.99. Whereas case 2 and case 3 have their highest values at the same conditions ( $Re_{hw}=2000 - Re_{cw}=8000$ ) of around 1.96 and 1.57 respectively. So, all the three cases have remarkable improvement however, case 1 witnessed the best improvement, where the maximum value of case 1 is the highest among the maximum values of case 2 and case 3, and the minimum value of case 1 is the highest over the minimum values of case 2 and case 3. This proves that case 1 design is the best design in order to obtain a good heat transfer enhancement. On the other side, case 2 shows acceptable results, where the ratio  $U/U_0$  reaches an average value of 1.55 for  $Re_{hw}=8000 - Re_{cw}=2000$  and 1.08 for  $Re_{hw}=2000 - Re_{cw}=8000$ , however the improvement is still less than case 1, which exhibits an average value of 1.73 for  $Re_{hw}=2000 - Re_{cw}=8000$

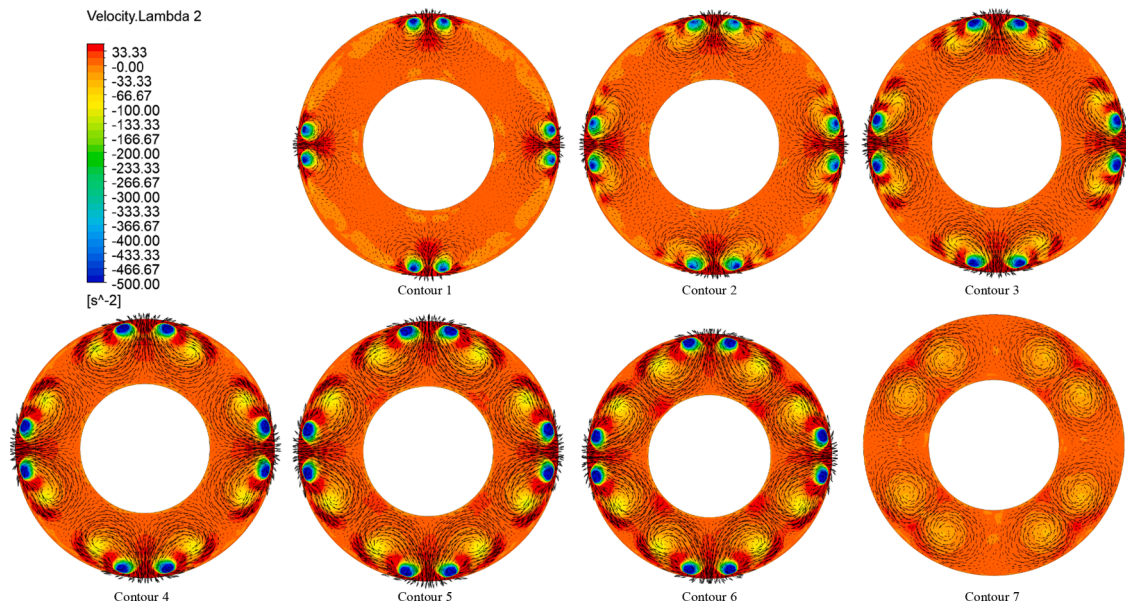


Fig. 15. Vortices profiles of case 3 for  $Re_{hw}=8000 - Re_{cw}=2000$ .

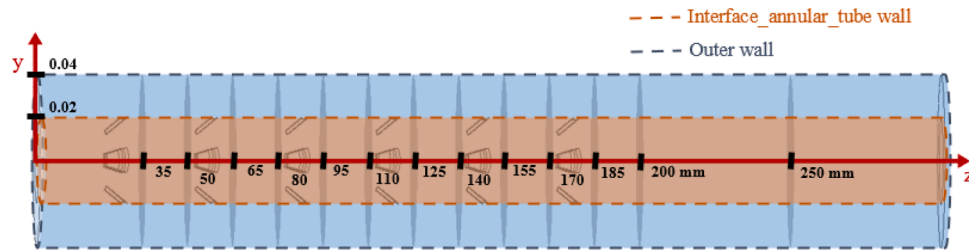


Fig. 16. Schematic of the design with the created planes.

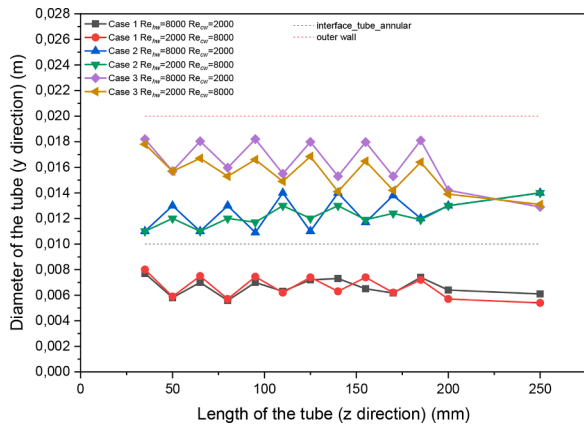


Fig. 17. Evolution of the vortices along the tube.

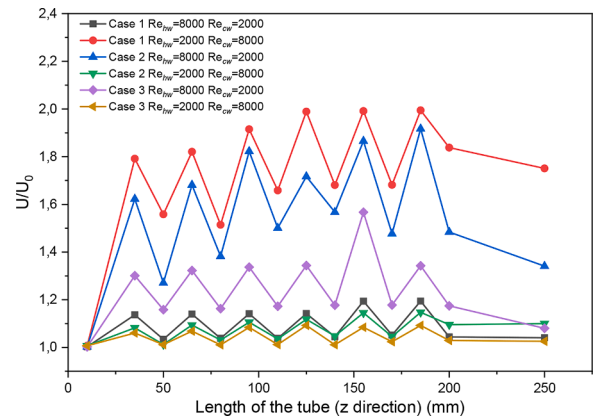


Fig. 18. Normalized overall heat transfer.

and 1.09 for  $Re_{hw}=8000 - Re_{cw}=2000$ . For case 3, there was modest improvement compared to the two previous cases, where the average ratio of  $U/U_0$  displays 1.24 for  $Re_{hw}=8000 - Re_{cw}=2000$  and 1.04 for  $Re_{hw}=2000 - Re_{cw}=8000$ , thus even with this slight improvement VGs enhances the heat transfer.

From Fig. 18, it can be observed that the installation of VGs on the inner tube is advantageous to enhance heat transfer than others with a lower flow rate of hot fluid than cold fluid. this could be attributed to the geometrical shape of the tube that help the vortices to reenergize, where the concave surface of the tube allows the vortices to grow thus having

larger heat transfer effect as shown in the Fig. 19, where the red points indicate the location of the center of vortices along the tube as it flows for high improvement of case 1  $Re_{hw}=2000 - Re_{cw}=8000$ . On the other side, the convex shape of the annular made the vortices dissipate leaving small effect on heat transfer as noticed in Fig. 19, where the blue points indicate the location of the center of vortices along the annular as it flows for high improvement of case 2  $Re_{hw}=8000 - Re_{cw}=2000$ . That explains why the vortices inside the tube will yield higher  $q$  than vortices located in the annular region.

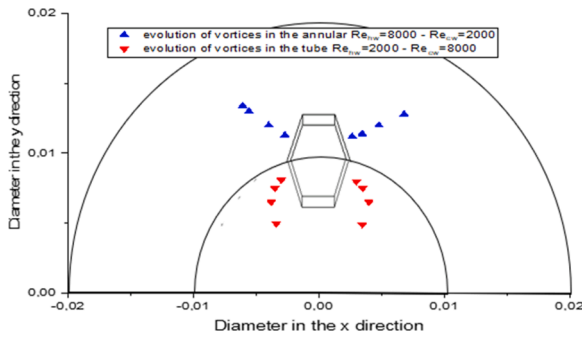


Fig. 19. Center of the vortices along the tube and the annular for the optimum values of cases 1 and 2.

## 5. Conclusions

In this study, the impact of using vortex generators on the heat transfer in a Concentric Tube Heat Exchanger is numerically investigated. The simulation analysis is held on three different cases of VGs in different locations to study the spatial impact of the VGs on the enhancement of heat transfer. Thus, the heat transfer in each case is affected by two criteria: (1) geometry, which is the location of the VGs, and (2) Reynolds number in the annular and the tube. In general, results show that VGs enhance heat transfer in all the cases as shown by the evolution of vorticity and the local  $U/U_0$  ratio.

In case 1, VGs have the highest improvement, where the  $U/U_0$ ,  $q/q_0$ , and TEF reaches 195%, 202%, and 97% respectively. Besides, results show that the turbulence flow occurred in both parts tube and annular with higher turbulence in the hot region, which is effective to enhance heat transfer more than being in the cold region. This is approved by achieving the highest improvement at the operating conditions ( $Re_{hw}=2000 - Re_{cw}=8000$ ) when VGs are inside the tube and at ( $Re_{hw}=8000 - Re_{cw}=2000$ ) when VGs are in the annular; in both cases turbulence occurs in both parts to achieve desirable results. Case 1 and case 2 are found to be efficient as they achieved higher improvements compared to case 3. In more detail, the following points were concluded.

- The input pumping power that provides high Reynolds number should be invested in the region where there are no VGs. Thus, the flow at the part with VGs will be turbulent due to the presence of the turbulators represented by VGs, whereas, the flow in the region that has no VGs will be fluctuated due to the high Reynolds number that causes the flow to oscillate.
- VGs should be on the interface wall between tube and annular (where heat transfer occurs) to achieve higher results. At the outer wall, the advantage that VGs provide is much lower since the wall condition is adiabatic.
- The presence of multi rows of VGs regenerates vorticity, consequently, enhances heat transfer, where the behavior of the changes after each row of VG.

In case 1:

- Heat transfer was efficient at the condition ( $Re_{hw}=2000 - Re_{cw}=8000$ ) because a high Reynolds number causes higher velocity, consequently increasing the turbulent kinetic energy in the annular, with the presence of VGs in the tube, turbulence occurs as well even at a low Reynolds number. However, heat transfer is not very efficient at the operating condition ( $Re_{hw}=8000 - Re_{cw}=2000$ ) because the turbulence created from high Reynolds number in the tube is useless as vortices are already created due to the presence of VGs. Besides, the flow in the annular part is kept laminar.

In case 2:

- Similarly, heat transfer was efficient when the turbulence occurred in both regions, which means at condition ( $Re_{hw}=8000 - Re_{cw}=2000$ ). However, heat transfer is not very efficient at ( $Re_{hw}=2000 - Re_{cw}=8000$ ), because the turbulence created from high Reynolds number in the annular is useless as vortices are already created due to the presence of VGs. Besides the flow in the tube part was kept laminar.

In case 3:

- Concerning case 3, it is studied just at the highest point for which turbulence occurred in both parts tube and annular ( $Re_{hw}=8000 - Re_{cw}=2000$ ). However, the turbulence is on the outer side (adiabatic part) which makes the presence of VGs not very efficient as compared to case 1 and case 2.

Consequently, high vorticity in the annular or the tube alone is not enough to deliver better performance as shown in case 1 ( $Re_{hw}=8000 - Re_{cw}=2000$ ) or case 2 ( $Re_{hw}=2000 - Re_{cw}=8000$ ). Besides, extremely high vorticity in one region with turbulence created from the Reynolds number in the other one is not enough as well as illustrated in case 1 ( $Re_{hw}=8000 - Re_{cw}=8000$ ) or case 2 ( $Re_{hw}=8000 - Re_{cw}=8000$ ). Hence, the best performance occurred at the relative presence of vorticity and turbulence in both regions in case 1 ( $Re_{hw}=2000 - Re_{cw}=8000$ ) or case 2 ( $Re_{hw}=2000 - Re_{cw}=8000$ ), where turbulence evenly moves the flow, consequently, maintaining a homogeneous mixture which is favorable for the heat transfer enhancement.

Now, among case 1 ( $Re_{hw}=2000 - Re_{cw}=8000$ ) and case 2 ( $Re_{hw}=2000 - Re_{cw}=8000$ ), case 1 is slightly more efficient due to the structure of the turbulence in the hot flow that completely mixes the hot flow, where the presence of VGs generate specific nature of vortices that mingle the flow.

So, as a conclusion having turbulence in the annular due to the high  $Re$  number which is 8000 and turbulence in the tube due to the presence of VGs with a specific  $Re$  number in the laminar phase which 2000 shows the best performance for our case study.

## Declaration of Competing Interest

The authors declare that they have no known competing financial interests or personal relationships that could have appeared to influence the work reported in this paper.

## Data availability

The authors are unable or have chosen not to specify which data has been used.

## References

- [1] Karthik Silaipillayarputhur, Tawfiq Al Mughanam, Abdulaziz Al Mojil, Mohammed Al Dhmoush, Analytical and numerical design analysis of concentric tube heat exchangers – a review, *Mater. Sci. Eng.* 345 (2017), 012006.
- [2] Yikai Wang, Shuo Zong, Yulong Song, Feng Cao, Yaling He, Qiang Gao, Experimental and techno-economic analysis of transcritical CO<sub>2</sub> heat pump water heater with fin-and-tube and microchannel heat exchanger, *Appl. Therm. Eng.* 199 (2021), 117606.
- [3] Taraprasad Mohapatra, Biranchi N.Padhi, Sudhansu S.Sahoo, Rudra N.Pramanik, Performance analysis of three fluid heat exchanger used in solar flat plate collector system, *Energy Procedia* 109 (2017) 322–330.
- [4] Edreis Edreis, A. Petrov, Types of heat exchangers in industry, their advantages and disadvantages, and the study of their parameters, *Mater. Sci. Eng.* 963 (2020), 012027.
- [5] M. Farnam, M. Khoshvaght-Aliabadi, M.J. Asadollahzadeh, Heat transfer intensification of agitated U-tube heat exchanger using twisted-tube and twisted-tape as passive techniques, *Chem. Eng. Process. - Process Intensification* 133 (2018) 137–147.

- [6] Rohit S. Khedkar, Shriram S. Sonawane, Kailas L. Wasewar, Water to nanofluids heat transfer in concentric tube heat exchanger: experimental study, *Procedia Eng.* 51 (2013) 318–323.
- [7] Charbel Habchi, Akram Ghanem, Thierry Lemenand, Dominique Della Valle, Hassan Peerhossaini, Mixing performance in split-and-recombine milli-static mixers—a numerical analysis, *Chem. Eng. Res. Design* 142 (2019) 289–306.
- [8] Ramin Zarei, Kiyanoosh Razzaghi, Farhad Shahraki, Experimental study of flow and thermal behaviour in single and multi-pass chevron-type plate heat exchangers, *Chem. Eng. Processing - Process Intensification\** 166 (2021), 108508.
- [9] Akram Ghanem, Charbel Habchi, Thierry Lemenand, Dominique Della Valle, Hassan Peerhossaini, Mixing performances of swirl flow and corrugated channel reactors, *Chem. Eng. Res. Design* 92 (11) (2014) 2213–2222.
- [10] Akshaykumar Magadam, Aniket Pawar, Rushikesh Patil, Rohit Phadtare, T. C Mestri, Experimental investigation of parallel and counter flow heat exchanger, *Int. J. Adv. Res. Sci. Eng. Technol.* 3 (3) (2016) 1610–1615.
- [11] Vinous M. Hameed, Fatima J. Hamad, Implementation of novel triangular fins at a helical coil heat exchanger, *Chem. Eng. Process. - Process Intensification* 172 (2022), 108745.
- [12] Rima Aridi, Jalal Faraj, Samer Ali, Thierry Lemenand, Mahmoud Khaled, Thermoelectric power generators: state-of-the-art, heat recovery method, and challenges, *Electricity* 2 (3) (2021) 359–386.
- [13] Rima Aridi, Jalal Faraj, Samer Ali, Mostafa Gad El Rab, Thierry Lemenand, Mahmoud Khaled, Energy recovery in air conditioning systems: comprehensive review, classifications, critical analysis, and potential recommendations, *Energies* 14 (18) (2021) 5869.
- [14] Hui Xiao, Zhimin Dong, Rui Long, Kun Yang, Fang Yuan, A study on the mechanism of convective heat transfer enhancement based on heat convection velocity analysis, *Energies* 12 (2019) 4175.
- [15] Qinfu Hou, Jieqing Gan, Zongyan Zhou, Aibing Yu, Particle scale study of heat transfer in packed and fluidized beds, *Adv. Chem. Eng.* 46 (2015) 193–243.
- [16] H. Karkaba, T. Dbouk, C. Habchi, S. Russeil, T. Lemenand, D. Bougeard, Multi objective optimization of vortex generators for heat transfer enhancement using large design space exploration, *Chem. Eng. Process. - Process Intensification* 154 (2020), 107982.
- [17] Assadour Khanjian, Charbel Habchi, Serge Russeil, Daniel Bougeard, Thierry Lemenand, Effect of the angle of attack of a rectangular wing on the heat transfer enhancement in channel flow at low Reynolds number, in: *Heat Mass Transfer*, 54, 2018, pp. 1441–1452.
- [18] Hefang Deng, Jinfang Teng, Mingmin Zhu, Xiaoqing Qiang, Shaopeng Lu, Yuting Jiang, Overall cooling performance evaluation for film cooling with different winglet pairs vortex generators, *Appl. Therm. Eng.* 201 (2022), 117731.
- [19] Markus Rutten Lars Krenkel, Heat transfer enhancement by using vortex generators, in: *8th. World Congress on Computational Mechanics (WCCM8)*, Venice, Italy, 2008.
- [20] Fachun Liang, Guoxiang Tang, Changyi Xu, Chi Wang, Zhengyu Wang, Jiabin Wang, Naiming Li, Experimental investigation on improving the energy separation efficiency of vortex tube by optimizing the structure of vortex generator, *Appl. Therm. Eng.* 195 (2021), 117222.
- [21] S. Ali, C. Habchi, T. Lemenand, J.L. Harion, Towards self-sustained oscillations of multiple flexible vortex generators, *Fluid Dyn. Res.* 51 (2) (2019), 025507.
- [22] S. Ali, C. Habchi, S. Menanteau, T. Lemenand, J.L. Harion, Three-dimensional numerical study of heat transfer and mixing enhancement in a circular pipe using self-sustained oscillating flexible vorticity generators, *Chem. Eng. Sci.* 162 (2017) 152–174.
- [23] Samer Ali, Sébastien Menanteau, Charbel Habchi, Thierry Lemenand, Jean-Luc Harion, Heat transfer and mixing enhancement by using multiple freely oscillating flexible vortex generators, *Appl. Therm. Eng.* 105 (2016) 276–289.
- [24] S. Ali, C. Habchi, S. Menanteau, T. Lemenand, J.L. Harion, Heat transfer and mixing enhancement by free elastic flaps oscillation, *Int. J. Heat Mass Transf.* 85 (2015) 250–264.
- [25] Monica Syaiful, M.S.K. Pranita Hendraswari, S.U. Tony, Maria F. Soetanto, Heat transfer enhancement inside rectangular channel by means of vortex generated by perforated concave rectangular winglets, *Fluids* 6 (43) (2021).
- [26] Thierry Lemenand, Charbel Habchi, Dominique Della Valle, Hassan Peerhossaini, Vorticity and convective heat transfer downstream of a vortex generator, *Int. J. Therm. Sci.* 125 (2018) 342–349.
- [27] M. Bayareh, M.N. Ashani, A. Usefian, Active and passive micromixers: a comprehensive review, *Chem. Eng. Process. - Process Intensification* (2019), 107771.
- [28] Mattia Samiolo, Patrick G. Verdin, Numerical modelling of a finless heat exchanger layout for electric vehicle application, *Appl. Therm. Eng.* 211 (2022), 118506.
- [29] G.N.a.S. Kleiin, *Introduction to Engineering Heat Transfer*, Cambridge University Press, United Kingdom, 2021.
- [30] F.R. Menter, Two-equation eddy-viscosity turbulence models for engineering applications, *AIAA J.* 32 (8) (1994) 1598–1605.
- [31] "ANSYS Academic Research, Release 15.0, Help System, User's Guide, ANSYS, Inc."
- [32] R.F. Warming, Richard M. Beam, Upwind second-order difference schemes and applications in aerodynamic flows, *AIAA J.* 14 (9) (1976) 1241–1249.
- [33] Dawid Taler, Jan Taler, Simple heat transfer correlations for turbulent tube flow, in: *E3S Web of Conferences*, 2017.
- [34] J.J. Lorenz, D.T. Yung, C.B. Panchal, G.E. Layton, An Assessment of Heat-Transfer Correlations For Turbulent Water Flow through a Pipe at Prandtl Numbers of 6.0 and 11.6, U. S. Department of Energy, United States, 1982.
- [35] J. Jeong, F. Hussain, On the identification of a vortex, *J. Fluid Mech.* 285 (1995) 69–94.